Appendix for "Transmission potential of human schistosomes is driven by resource competition among snail intermediate hosts"

David J. Civitello, Karena H. Nguyen, Rachel B. Hartman, Andres Manrique, Bryan K. Delius, LM Bradley, Roger M. Nisbet, and Jason R. Rohr

Appendix contents

Scenario description and individual-based model overview

The simulations presented here correspond to the design of the mesocosm experiment and aim to represent ecologically realistic scenarios of seasonal schistosome transmission sites, e.g. (1, 2). Simulations were initialized with conditions reflecting the design of the mesocosm experiment, i.e., an initial a population of 60 snails in a 500-L environment and continued for 120 days. Miracidia were introduced at a constant-daily introduction rate, transmission parameters were estimated from experimental exposures (3), and host and parasite dynamic energy budget (DEB) parameters were estimated from experiments on manipulated resource supply rates and periodic starvation periods (4).

Simulation schedule

We implemented the model with discrete daily time steps. We initialized the snail populations with 60 individuals, with body lengths drawn from a uniform distribution ranging from 2 – 16 mm. Initially, the environment has an algal resource density of 1 mg Carbon L^{-1}, and

no miracidia or cercariae. At the beginning of each step, miracidia are introduced into the water and a discrete stochastic transmission model determines if any snails become infected by the population of free-living schistosome miracidia. The transmission model explicitly represents exposure (irreversible contact) and infection probability given exposure for each miracidium. Miracidia that fail to contact a snail may survive to the next day. All miracidia that fail to infect following a contact die. Successful infections add parasite biomass to an individual snail's DEB model. Next, each susceptible and infected snail follows its own DEB model for resource consumption, growth, reproduction, survival, and production of parasite cercariae (4-6). Algal resources grow logistically and are consumed by all snails in the population. The DEB and resource models are integrated over the duration of the time step. If, over a timestep, a snail has allocated sufficient energy to produce a whole number of eggs or cercariae, they are released into the environment on the day of production. The survival of each snail is then determined as a probabilistic outcome based on the snail's current mortality hazard. Snail eggs hatch with a 10-day time lag from laying date, contributing new individuals (with initial length 0.75 mm) to the population. Finally, all snail and environmental quantities are updated at the end of each daily step.

Full description of the individual-based model of algae-snail-schistosome dynamics

We previously built an individual-based epidemiological model for the human schistosome, *S. mansoni*, infecting a size-structured *B. glabrata* host population (7, 8). The model is composed of three connected submodules: 1) a within-host dynamic energy budget (DEB) model for *B. glabrata* host biomass and *S. mansoni* parasite biomass (4-6), 2) a between-host transmission model that describes infection following contact between hosts and

schistosome miracidia, the free-living life stage, excreted by humans into freshwater environments of miracidia and snails (3), and 3) a resource production model representing logistically growing periphytic algae.

Within-host dynamic energy budget and resource production model

The DEB model used to represent each snail builds on the "standard model" of DEB theory (9). It uses ordinary differential equations to track changes in the density of logistically-growing food resources, F, in the environment shared by all snails (with each snail distinguished with the subscript *i)* as well as several host traits: physical length, L_i (shell diameter; assumed to be proportional to the cube root of structural biomass); the scaled density of energy reserves, e_i; and resources that have been committed to development, D_i, or reproduction, R_{Hi}. We extended the standard DEB model by adding two modules that track a within-host population of parasites and host survival, respectively. Within each host, we track the change in parasite biomass, P_i, and the resources that have been invested in parasite reproduction, R_{Pi}. To model mortality, we introduced a variable represented the scaled density of repairable "damage", δ, as well as an instantaneous hazard rate for mortality, H_i, which increases proportionally to damage. The model structure is presented in Equations 1 – 10 below. State variables, parameters are listed in Table S1. Several derived parameters, functions, or equalities simplify the presentation of the model and are also listed in Table S1. Subscripts H and P distinguish host and parasite variables and parameters. All parameter values used in this simulation study are defined in Table S2. Overall, this model generically represents the consumption of host energy for growth and the production and release of infectious propagules while providing a parsimonious description of prominent phenomena in snail-schistosome physiology, e.g., potential for reproductive manipulation,

castration, and gigantism. A full derivation of the survival module along with discussion and justification of the parasitism module are presented in (4, 5).

$$\frac{dF}{dt} = r\left(1 - \frac{F}{K}\right) - i_M f_H \sum_i^N L_i^2 \quad \text{(Eq. 1)}$$

$$\frac{dL_i}{dt} = \frac{gY_{VE}}{3\chi}\left(\frac{\kappa_i^* a_M e_i - (m_V + m_R E_M \delta_i)\chi L_i}{g + e_i}\right) \quad \text{(Eq. 2)}$$

$$\frac{de_i}{dt} = \frac{a_M}{\chi E_M L_i}(f_H - e_i) - \frac{i_{PM} f_P P_i}{E_M \chi L_i^3} \quad \text{(Eq. 3)}$$

$$\frac{dD_i}{dt} = \begin{cases} (1-\kappa_i^*)C - m_D D_i & if\ D_i < D_R \\ \min\left((1-\kappa_i^*)C - m_D D_i, 0\right) & if\ D_i \geq D_R \end{cases} \quad \text{(Eq. 4)}$$

$$\frac{dR_{Hi}}{dt} = \begin{cases} 0 & if\ D_i < D_R \\ \max\left((1-\kappa_i^*)C - m_D D_i, 0\right) & if\ D_i \geq D_R \end{cases} \quad \text{(Eq. 5)}$$

$$\frac{dP_i}{dt} = (Y_{PE} i_{PM} f_P (1 - r_{Pi}) - m_P) P_i \quad \text{(Eq. 6)}$$

$$\frac{dR_{Pi}}{dt} = \gamma_{RP} Y_{PE} i_{PM} f_P r_{Pi} P_i \quad \text{(Eq. 7)}$$

$$\frac{d\delta_i}{dt} = \frac{\Theta}{\chi L_i^3}\frac{dR_{Pi}}{dt} + k_R(1 - e_i) - k_R \delta_i - \frac{3\delta_i}{L_i}\frac{dL_i}{dt} \quad \text{(Eq. 8)}$$

$$\frac{dH_i}{dt} = h_b + h_\delta max(\delta_i - \delta_0, 0) \quad \text{(Eq. 9)}$$

$$Prob(Survival)_i[t] = e^{-H_i(t)} \quad \text{(Eq. 10)}$$

Snail hosts consume logistically growing algal food resources, F, with a Type-II scaled functional response, f_H, with half saturation constant, F_h, and a surface area (L_i^2)-dependent maximum ingestion rate, i_M (Eq. 1; Table S1). Logistic growth of algal resources and consumption of algae by the snail population fully specifies the resource production module of

the IBM. Hosts assimilate food into energy reserves, with yield Y_{EF}. The maximum assimilation rate, a_M, is the product of the maximum ingestion rate and the yield of reserves on food. Hosts use reserve energy to build two types of biomass: somatic structure (which performs vital functions and requires maintenance at rate m_V), and reproductive matter (reserve which has been irreversibly committed to gametes). Reserve mobilization increases linearly with reserve density (9). Hosts allocate a constant portion, κ, of mobilized reserves, C_i, to somatic (vs. reproductive) processes. Hosts grow in length based on the yield of structure on reserves, Y_{VE}, and the energy mobilized for somatic processes minus the costs of somatic maintenance and repair (Eq. 2). Juveniles use energy allocated to "reproduction" for development, D_i (Eq. 4). Reproduction begins after maturing above the developmental threshold for reproduction, D_R, and developmental status requires maintenance at the specific rate m_D.

If infected, a population of parasites grows within the host and consumes host reserves (Eq. 3). Parasite biomass, P_i, (Eq. 6) increases through parasite ingestion and assimilation of host reserves, also following a Type-II scaled functional response, f_P, with a half saturation coefficient, e_h, maximum mass-specific ingestion rate, i_{PM}, and yield of parasite biomass on host reserve, Y_{PE}. Parasite biomass requires maintenance at mass-specific rate m_P. A proportion, r_{Pi}, of the assimilated reserve is allocated to parasite reproduction, while the rest is allocated to parasite biomass growth. The allocation proportion r_{Pi} itself increases as a sigmoid function of parasite density within the physical volume of the snail host's shell, with an inflection point at p_h (Table S1), reflecting within-host density dependence in parasite growth. Biomass of parasite offspring (cercariae) increases from parasite allocation to reproduction, with the relative yield of parasite reproduction biomass on assimilated reserve, γ_{RP}. Infection can also alter the host's realized allocation between soma and reproduction, κ_i*, with parasite density dependent

manipulation rate, α, yielding an effective allocation rule, $\kappa_i^* = \min(\kappa + \alpha P_i, 1)$. This expression, using the minimum function, represents the assumption that increased parasite biomass increases the somatic allocation proportion, but, by definition as a proportion, this allocation fraction can never exceed 1. Schistosome infection increases κ_i^* in snails, therefore it can cause parasitic castration, the rapid termination of reproduction by infected hosts, and host gigantism, the temporarily increased growth of infected hosts relative to uninfected hosts, phenomena that are prominent in snail-trematode interactions and also seen across a variety of host-parasite systems (10, 11).

Resource consumption by parasites and uninfected competitors can cause focal hosts to starve, therefore, we incorporated a "shrinking and regression" rule to describe the physiological consequences of hosts being unable to pay somatic or reproductive maintenance costs. Snails lose structural mass (although their shells do not shrink) if reserves mobilized to soma cannot cover somatic maintenance. Similarly, hosts halt reproduction and regress developmentally if reserves mobilized to reproduction are insufficient to pay for developmental maintenance (4).

Hosts die at a background rate and from damage caused by low energy reserve density or emerging parasite offspring. Scaled damage density, δ_i, increases due to the release of parasite offspring with damage intensity, Θ. The damage repair rate, k_R, determines the rate of damage caused by reserve depletion and damage repair. Damage density also decreases through dilution by growth and may be concentrated by shrinkage (Eq. 8). Snail hosts can repair damage, which requires energy, and we assume that these costs, m_R, are an explicit portion of somatic maintenance (i.e., these costs must be paid fully before mobilized reserves can fuel somatic growth). Cumulative hazard, H_i, increases with the background hazard rate, h_b, and a linear function of damage density above a threshold, δ_0, with hazard coefficient h_δ (Eq. 9). Host

142 survival probability, $Prob(Survival[t])_i$ is a negative exponential function of cumulative hazard,
143 H_i, (Eq. 10).

144 Between host transmission model

145 Snail hosts can be infected following density-dependent contact with free-living
146 miracidia following a model that separates the transmission process into two components:
147 irreversible exposure of hosts to parasites in the water (i.e., invasion of host tissues by a parasite,
148 at rate ε) and a per miracidium probability of infection given exposure, σ (3). We assume that
149 miracidia are introduced into the aquatic environment at a constant daily rate, M_{in}, and that
150 parasites in the water die at a background mortality rate, m_M. A successful snail infection adds
151 the carbon biomass of a single miracidium (2.85×10^{-5} mg C) to the parasite biomass
152 compartment, P_i, of that specific host's DEB model (Eq. 6). If the host was previously
153 uninfected, this event can effectively be viewed as "turning on" the parasite submodel within the
154 energy budget. Thereafter, within-host energy consumption, parasite biomass accumulation,
155 parasite reproduction, and parasite-mediated damage can occur. The transmission is implemented
156 as a stochastic realization of a single day simulation within the IBM at the start of each daily
157 time step. For each miracidium present in the water, there are three potential outcomes: 1)
158 successful snail infection, 2) death following host infection or in the water, or 3) survival in the
159 water until the next day. Given these parameters, along with densities of snail hosts, *S*, and
160 miracidia, *M*, the transmission model implies the following probability that a miracidium infects
161 snail *i* in a time interval spanning time = 0 through time = *t*.

162 $$Probability(Infection)[t]_i = \frac{\sigma\varepsilon}{m_M+\varepsilon S} 1 - e^{-(\varepsilon S+d_M)t} \quad \text{(Eq. 11)}$$

163 We note first that here, *e*, represents Euler's constant, and not e_i, the scaled reserve density of
164 snail *i*. Second, this representation, where snail infection probability is a decreasing function of

snail density, *S*, reflects the biological reality that irreversible exposure (regardless of infection success or failure) removes parasites from the environment and that any one parasite can only invade a single host (3).

Some parasites that do not invade a snail host can survive to the next daily time step. The transmission model implies the following probability for this occurrence:

$$Probability(Miracidium\ surives\ in\ the\ water)[t] = e^{-(\varepsilon S + m_M)t} \quad \text{(Eq. 12)}$$

Again, in this equation, *e*, represents Euler's constant, and not e_i, the scaled reserve density of snail *i*.

Miracidia that fail to infect a snail following irreversible exposure or to survive in the aquatic environment die. The transmission model implies the following probability for miracidial mortality in a time interval spanning time = 0 through time = *t*:

$$Probability(Miracidium\ dies)[t] = \left(\frac{m_M}{m_M+\varepsilon S} + \frac{(1-\sigma)\varepsilon S}{m_M+\varepsilon S}\right)\left(1 - e^{-(\varepsilon S + m_M)t}\right) \quad \text{(Eq. 13)}$$

In Eq. 13 the two terms within the first quantity represent the two different sources of mortality, death in the water without invading a snail and death after snail invasion, respectively. The second quantity represents the probability of a miracidium not remaining alive in the water at time *t*. Formally, this expression could be simplified by combining these terms, but we retain this presentation to make the biological interpretation more apparent.

The stochastic outcome of a single timestep of the transmission module occurs by simulating a single draw from a multinomial distribution where the probability of "success" for all events are described as above and the number of "trials" is equal to the number of miracidia in the environment.

<u>Susceptible-Exposed-Infectious model of snail-schistosome dynamics</u>

We contrast the predictions and assumptions of the DEB-based IBM against an Susceptible-Exposed-Infectious (SEI) model of snail-schistosome dynamics that ignores the effect of resources of the production of schistosome cercariae. There is no singular model that is uniformly applied to schistosome transmission dynamics. However, many widely used models are variations on a core structure that represent several assumptions: 1) snail populations grow logistically (i.e., there is implicit competition among snail hosts that reduces per capita reproductive rates), 2) snail infections arise from density-dependent transmission following contact with miracidia. However, sometimes miracidia are abstracted away from these models and the transmission rate to snails is considered to depend on the density of susceptible snails and the number of adult worms within human hosts. Formally, this introduces the additional assumption that per-schistosome reproduction within humans is density independent, 3) snails transition from the susceptible class to the exposed class (reflecting pre-patent (i.e., non-shedding infections). After the pre-patent period, snails transition from the exposed class to the infectious class, 4) infectious snails release cercariae at a constant rate and suffer the virulent effects of schistosome infection; reduced survival and fecundity, and 5) transmission rate to humans depends on the density of cercariae and humans. Again, because of the assumption that all infectious snails release cercariae at a constant rate, cercariae are often abstracted out of these models, and transmission rate to humans is considered to depend on the density of infectious snails and humans. Taking these assumptions together yields a generic SEIC (Susceptible-Exposed-Infectious-Cercariae) model for snail-schistosome dynamics that represents the dominant perspective of the aquatic ecology of schistosomes:

$$\frac{dS}{dt} = b\left(1 - \left(\frac{(S+E+I)}{K}\right)\right)(S+E) - mS - \beta MS \qquad \text{(Eq. 14)}$$

$$\frac{dE}{dt} = \beta MS - (m + \sigma)E \quad \text{(Eq. 15)}$$

$$\frac{dI}{dt} = \sigma E - (m + m_I)I \quad \text{(Eq. 16)}$$

$$\frac{dC}{dt} = \lambda I - m_C \mathrm{C} \quad \text{(Eq. 17)}$$

Snails reproduce negative density dependence, resulting in logistic population growth with maximum per capita reproduction rate, *b*, and carrying capacity, *K* (Eq. 14). Only susceptible, *S*, and exposed, *E*, snails reproduce, as schistosome infections castrate infectious snails, *I*. All snail hosts regardless of infection status contribute to competitive effects on reproduction. Susceptible snails die, at background mortality rate *m*, and they become infected upon density dependent infection with miracidia. Here we represent a constant introduction rate of miracidia by humans and all aspects of the ensuing transmission process with a single compound parameter, β*M*. Snails that have been successfully invaded by miracidia transition to the exposed class, *E*, and they die at the same background mortality rate as susceptible snails, *m*. Additionally, exposed (pre-patent) snails transition to the infectious (patent) class at a constant rate, σ (Eq. 15). Infectious snails die with an additional death rate due to schistosome infection, m_I (Eq. 16) and they release human-infectious cercariae into the environment at a constant per capita rate, λ (Eq. 17). Cercariae in the environment die at a constant death rate, m_C. All state variables and parameters are defined in Table S3.

Here we focus on the dynamics of snails and schistosomes and consider (as for the IBM) scenarios where introduction of miracidia occurs at a constant rate to focus on the "within season" aquatic dynamics and ecology of this system. We explicitly model cercarial dynamics to facilitate direct comparisons to predictions from the IBM. While this model is representative of generic aquatic dynamics that reflect past and current schistosomiasis modeling efforts, it is

232 important to acknowledge that there are a variety of important extensions and elaborations to
233 these models, especially those that consider variation in human demography, behavior, immune
234 status, and various control methods (12-14), which are all complementary to the focus on aquatic
235 dynamics presented here.
236
237 Additional simulation and discussion of the IBM
238 In Figure 1, we presented the dynamics resulting from a single run of the IBM to contrast
239 against the predictions generated by the SEI model. Here, we present additional simulation
240 results to evaluate whether the key predictions from the IBM are robust to 1) temporal variation
241 in miracidial introduction, and 2) variation to two key parameters, the rate of miracidial
242 introduction, M_{In}, and the maximum growth rate of algal resources, r.
243 First, we ran 50 replicate simulations as described in the main text (with a constant rate of
244 miracidial input; $M_{In} = 10\ d^{-1}$). We then ran another set of 50 simulations in which miracidia
245 were introduced to the environment on a biweekly schedule, as in the experiment, only on days
246 1, 15, 29, and 43. We set $M_{In} = 140\ d^{-1}$ on these four dates and we set $M_{In} = 0\ d^{-1}$ at all other
247 times to standardize the same input of miracidia over the first eight weeks of the simulation. We
248 then plotted the dynamics of snails, cercariae, and algal resources through time (Figure S1). The
249 main dynamics of these scenarios are extremely similar. Both predict an intense pulse in
250 cercarial production as snail populations grow followed by essentially no parasite release once
251 the snail populations suppress algal resources and begin to decline. The scenario representing
252 biweekly pulses of miracidial introduction caused a slight acceleration in the onset of the
253 cercarial pulse and an increase in the duration and peak of this pulse of cercarial density. This
254 occurred because this scenario caused snails to become infected slightly earlier on average,

thereby enabling snails to begin releasing cercariae earlier and with a longer period of time before snail suppression of algal resource availability and starvation-induced cessation of cercarial production.

Next, we retained the constant miracidial input rate M_{In}, and explored how variation in this rate and the growth rate of algal resources, r, affect the snail-schistosome dynamics predicted by the IBM. Over a gradient of $1 \leq M_{In} \leq 10000$ d^{-1}, the model predicts that increased miracidial introduction increases the number of infected snails and therefore the total production of schistosome cercariae (Figure S2). At all input rates, the model maintains the prediction of a cercarial pulse, in contrast to models that ignore the effects of resources on cercarial production. As the input rate increases, the pulse begins earlier in the season, reflecting the increasingly rapid infection of snails. At the highest input rates, a lower level of cercarial production is sustained late in the season. This effect occurs in these simulations because these input rates generate enormously high infection prevalence in snails, causing mortality and castration effects to regulate the snail population and increases *per capita* resource acquisition, and therefore cercarial production, for the few remaining snails, i.e., it causes a trophic cascade (15). This trophic cascade seems extremely ecologically unrealistic, as the prevalence of schistosome infections in snails is often extremely low (1-10%), even when prevalence in humans is high (16). In summary, across these parameter ranges, total cercarial production summed over the transmission season can be limited by miracidial input or resource productivity. However, within any scenario, cercarial production is limited at early time points by the density of infected snails and then at later time points by resource competition and the *per capita* production of cercariae.

Figure S1

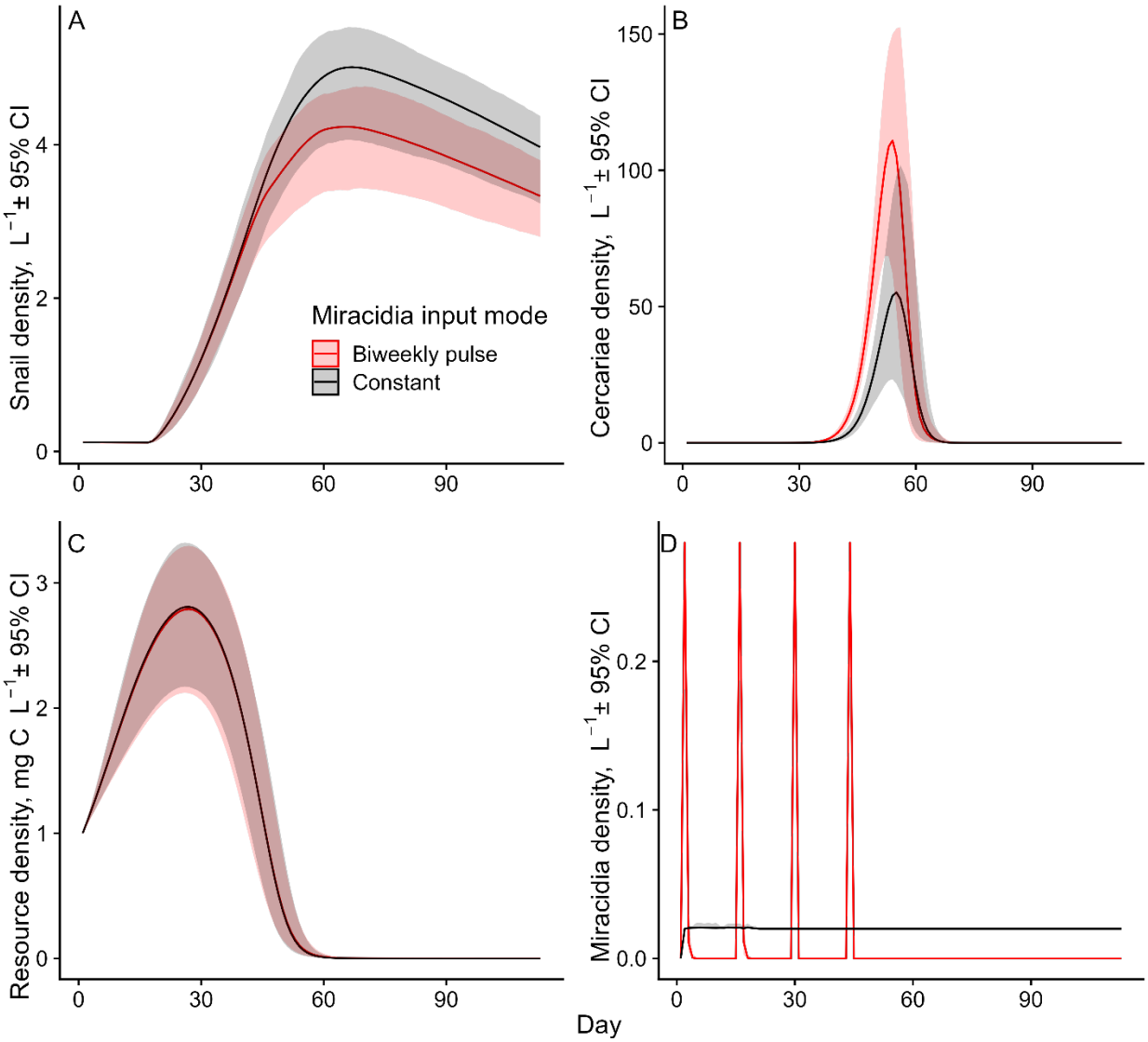

Figure S1. Simulated dynamics of (A) snails, (B) cercariae, and (C) algal resources from the IBM for seasonal transmission scenarios when miracidia are introduced at a constant daily rate (black) or in biweekly pulses (red) as in the experiment. Temporal variation in miracidial introduction caused little qualitative variation in predicted dynamics. There was a slight reduction in (A) snail density and a slight acceleration in (B) the onset of the cercarial pulse under the biweekly miracidia input mode. This arose because this parasite input scenario slightly accelerates host infection, e.g., because it supplies an equivalent number of parasites on day one as the total miracidia that are supplied on days 1-14 in the constant scenario. Lines represent mean dynamics and shaded regions represent 95% confidence intervals of sets of 50 simulation runs using these miracidia introduction scenarios and all other model parameters and processes as for Figure 1.

Figure S2

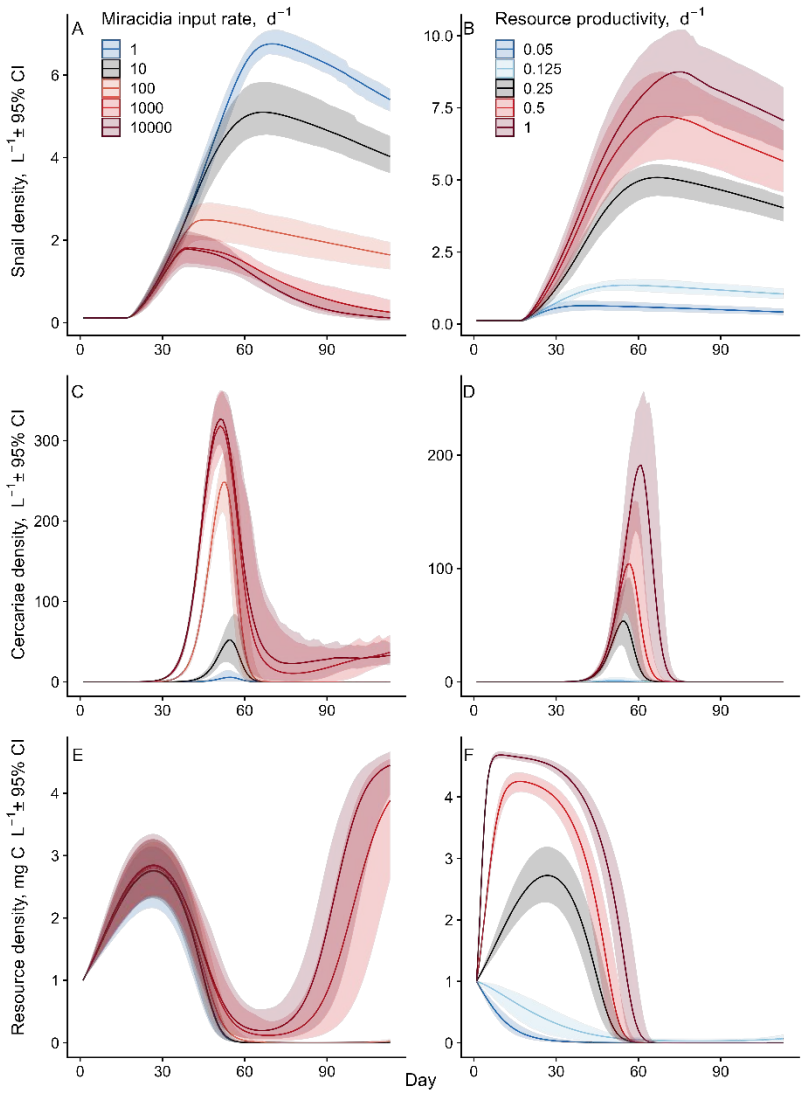

Figure S2. Simulated dynamics of (A, B) snails, (C, D) cercariae, and (E, F) algal resources from the IBM for seasonal transmission scenarios along gradients of miracidial input rate (left column) and maximum resource growth rate (right column). Increasing miracidial input rates cause more infection of snails, leading to earlier onset of the pulse of cercarial production and a larger and longer peak. Greater snail infection also suppresses snail density due to virulent effects on host survival and reproduction. Greater resource productivity causes larger snail populations and increases the peak and duration of the pulse in cercarial production. In all cases, when the parameter combination facilitated production of cercariae, there was a pronounced pulse of cercarial production as snail populations grew. Black color indicates the parameter values presented in the main text, red color indicates parameter values greater than those used in the main text, and blue color indicates parameter values that are less than those used in the main text. Lines represent mean dynamics and shaded regions represent 95% confidence intervals of sets of 50 simulation runs using these parameter values while maintaining all other model parameters and processes as for Figure 1.

Table S1. Parameters and compound functions for the bioenergetic model of within-host infection dynamics.

(A) State variables		
Quantity	Description	Units
F	Environmental resource abundance	mg C
L_i	Physical host length of snail *i*	mm
e_i	Scaled density of host energy reserves of snail *i*	dimensionless
D_i	Host reserve invested in maturity/development for snail *i*	mg C
R_{Hi}	Host reserve invested in reproduction for snail *i*	mg C
P_i	Parasite biomass in snail *i*	mg C
R_{Pi}	Parasite biomass invested in reproduction in snail *i*	mg C
(B) Primary parameters (Host)		
Quantity	Description	Units
i_M	Surface area-specific maximum host ingestion rate	mg C d^{-1} mm^{-2}
F_h	Host (Type-II) foraging half saturation constant	mg C
Y_{EF}	Yield of reserve on resources	dimensionless
Y_{VE}	Yield of structure on reserve	dimensionless
κ	Proportion of mobilized reserve allocated to soma	dimensionless
m_D	Maintenance rate for development/maturity	d^{-1}

L_M	Maximum physical host length	mm
χ	Ratio of structural biomass to physical length cubed	mg C mm^{-3}
E_M	Maximum host reserve biomass relative to structural biomass	dimensionless
D_R	Host maturity threshold for reproduction	mg C
ε_H	Carbon content of host offspring	mg C
(C) Primary parameters (Parasite)		
Quantity	Description	Units
Y_{AE}	Yield of parasite assimilate on host reserve	dimensionless
Y_{PA}	Yield of parasite biomass on assimilate	dimensionless
Y_{RP}	Yield of parasite offspring biomass on assimilate	dimensionless
i_{PM}	Parasite maximum mass-specific ingestion rate	mg C d^{-1}
e_h	Parasite ingestion half saturation constant	dimensionless
p_h	Parasite allocation half-saturation constant	dimensionless
α	Parasite manipulation of host allocation rule	mg C^{-1}
m_P	Mass-specific maintenance rate for parasites	d^{-1}
ε_P	Carbon content of parasite offspring	mg C
(D) Primary parameters (Damage, hazard, and survivorship)		
k_R	Damage repair rate constant	d^{-1}

Θ	Intensity of parasite-induced damage	dimensionless
h_b	Background hazard rate	d^{-1}
h_δ	Hazard coefficient of damage	d^{-1}
m_R	Scaled energy expenditure rate for damage repair	d^{-1}
δ_0	Damage density threshold	dimensionless

(E) Derived parameters and functions

Equation	Description	Units
$a_M = i_M Y_{EF}$	Maximum host assimilation rate	mg C d^{-1} mm^{-2}
$g = \frac{1}{\kappa^* Y_{VE} E_m}$	Cost of structural growth relative to maximum possible allocation to soma	dimensionless
$p_i = \frac{P_i}{\chi L_i^3}$	Parasite density in host structural tissue	dimensionless
$r_{Pi} = \frac{p_i^2}{{p_h}^2 + p_i^2}$	Proportional allocation of parasite assimilate to reproduction	dimensionless
$Y_{PE} = Y_{PA} Y_{AE}$	Yield of parasite biomass on host reserve	dimensionless

$\gamma_{RP} = \frac{Y_{RP}}{Y_{PA}}$	Relative yield of parasite reproduction on parasite assimilate	dimensionless
$C_i = \left(\frac{ge_i}{g + e_i}\right)\left(a_M L^2 + \frac{(m_V + m_R E_M \delta_i)\chi L_i^3}{\kappa_i^* g}\right)$	Commitment/mobilization rate of reserve	mg C d^{-1}
$m_V = \frac{\kappa a_M}{\chi L_M}$	Mass-specific maintenance rate for structure	d^{-1}
$\mu_D = \frac{m_D}{m_V}$	Scaled maturity maintenance rate	dimensionless
$M = \chi(1 + E_M)$	Volume-biomass coefficient for hosts	mg C mm^{-3}
$\kappa_i^* = min(\kappa + \alpha P_i, 1)$	Realized proportion of mobilized reserve allocated to soma	dimensionless
$f_H = \frac{F}{F_h + F}$	Scaled host functional response	dimensionless
$f_P = \frac{e_i}{e_h + e_i}$	Scaled parasite functional response	dimensionless

309

310

Table S2. Parameter estimates used in the IBM simulations

Parameter	Description	Estimate[1]	Units
Host parameters			
κ	Proportional allocation to soma	0.908	-
M	Mass:volume relationship	5.17×10^{-3}	mg C mm^{-3}
E_M	Maximum host reserve biomass relative to structural biomass	1.40	mg C
L_M	Maximum physical host length	53.6	mm
i_M	Surface area-specific maximum host ingestion rate	3.04×10^{-2}	mg C d^{-1} mm^{-2}
F_h	Host (Type-II) foraging half saturation constant	2	mg C L^{-1}
Y_{EF}	Yield of reserve on resources	0.269	-
Y_{VE}	Yield of structure on reserve	0.261	-
μ_D	Maintenance rate for maturity	0.133	-
D_R	Host maturity threshold for reproduction	0.617	mg C
ε_H	Carbon content of host offspring	0.015	mg C
hatch	Snail egg hatching probability	0.5	-
lag	Time lag for snail egg hatching	10	d
Parasite parameters			
α	Parasite manipulation of host allocation rule	2.20	mg C^{-1}
i_{PM}	Parasite maximum mass-specific ingestion rate	0.583	mg C d^{-1}
Y_{PE}	Yield of parasite biomass on reserve	0.937	-
e_h	Parasite ingestion half saturation constant	0.220	-
m_P	Mass-specific maintenance rate for parasites	0.311	d^{-1}
p_h	Parasite allocation half-saturation constant	0.128	-
Y_{RP}	Yield of parasite offspring biomass on assimilate	0.921	mg C
ε_P	Carbon content of parasite offspring	4×10^{-5}	mg C
Damage, hazard, survival, and repair parameters			
k_R	Damage repair rate constant	3.09×10^{-2}	d^{-1}
δ_0	Damage density threshold	2.61×10^{-2}	-
h_δ	Hazard coefficient of damage	4.73×10^{-3}	d^{-1}
h_b	Background hazard rate	3.09×10^{-4}	d^{-1}
Θ	Intensity of parasite-induced damage	79.3	-
m_R	Scaled energy expenditure rate for damage repair	8.06×10^{-6}	d^{-1}
Transmission model			
ε	Snail-miracidia contact rate	20	L d^{-1}
σ	Miracidia infection probability given contact	0.5	-
M_{in}	Miracidial input rate	10	d^{-1}
m_M	Mortality rate of miracidia	1	d^{-1}

Environmental/Resource parameters			
ENV	Volume of environment	500	L
r	Algal maximum growth rate	0.25	d^{-1}
K	Algal carrying capacity	5	mg C L^{-1}
M_Z	Mortality rate of cercariae	1	d^{-1}

1. Host, parasite, and damage, hazard, survival, and repair parameters derived from Civitello et al. 2020 and rounded to three significant figures.
2. Transmission model parameters rounded from estimates in Civitello and Rohr 2014
3. Environmental/resource parameters chosen to reflect a 500 L volume of habitat, realistic quantities of algal growth or detrital input, and rates of parasite mortality.

Table S3. State variables and parameters used in the SEIC simulations

Parameter	Description	Estimate	Units
State variables			
S	Susceptible snail density	-	L^{-1}
E	Exposed snail density	-	L^{-1}
I	Infectious snail density	-	L^{-1}
C	Cercarial density	-	L^{-1}
Parameters			
b	Maximum snail birth rate	0.1	d^{-1}
K	Snail carrying capacity	5	L^{-1}
βM	Miracidia introduction & snail transmission rate	0.01	d^{-1}
σ	Schistosome development rate to patency	0.036	d^{-1}
λ	Cercarial production rate	50	d^{-1}
m	Background mortality rate of snails	0.01	d^{-1}
m_I	Additional mortality rate of infectious snails	0.04	d^{-1}
m_C	Background mortality rate of cercariae	1	d^{-1}

1. D. Gurarie, C. H. King, N. Yoon, X. Wang, R. Alsallaq, Seasonal dynamics of snail populations in coastal Kenya: Model calibration and snail control. *Advances in Water Resources* **108**, 397-405 (2017).
2. J. Perez-Saez *et al.*, Hydrology and density feedbacks control the ecology of intermediate hosts of schistosomiasis across habitats in seasonal climates. *Proceedings of the National Academy of Sciences* **113**, 6427-6432 (2016).
3. D. J. Civitello, J. R. Rohr, Disentangling the effects of exposure and susceptibility on transmission of the zoonotic parasite Schistosoma mansoni. *Journal of Animal Ecology* **83**, 1379-1386 (2014).
4. D. J. Civitello, L. H. Baker, S. Maduraiveeran, R. B. Hartman, Resource fluctuations inhibit the reproduction and virulence of the human parasite *Schistosoma mansoni* in its snail intermediate host. *Proceedings of the Royal Society B: Biological Sciences* **287**, 20192446 (2020).
5. D. J. Civitello, H. Fatima, L. R. Johnson, R. M. Nisbet, J. R. Rohr, Bioenergetic theory predicts infection dynamics of human schistosomes in intermediate host snails across ecological gradients. *Ecology Letters* **21**, 692-701 (2018).
6. D. J. Civitello, R. B. Hartman, Size-asymmetric competition among snails disrupts production of human-infectious Schistosoma mansoni cercariae. *Ecology* **102**, e03383 (2021).
7. M. Malishev, D. J. Civitello, Linking bioenergetics and parasite transmission models suggests mismatch between snail host density and production of human schistosomes. *Integrative and comparative biology* **59**, 1243-1252 (2019).
8. M. Malishev, D. J. Civitello, Modelling how resource competition among snail hosts affects the molluscicide frequency and intensity needed to control human schistosomes. *Functional Ecology* https://doi.org/10.1111/1365-2435.13602 (2020).
9. S. Kooijman, *Dynamic energy budget theory for metabolic organisation* (Cambridge university press, 2010).
10. S. R. Hall, C. Becker, C. E. Cáceres, Parasitic castration: a perspective from a model of dynamic energy budgets. *Integrative and Comparative Biology* **47**, 295-309 (2007).
11. K. D. Lafferty, A. M. Kuris, Parasitic castration: the evolution and ecology of body snatchers. *Trends in parasitology* **25**, 564-572 (2009).
12. D. Gurarie *et al.*, Modelling control of Schistosoma haematobium infection: predictions of the long-term impact of mass drug administration in Africa. *Parasites & Vectors* **8**, 529 (2015).
13. M. E. J. Woolhouse, P. Taylor, D. Matanhire, S. K. Chandiwana, Acquired immunity and epidemiology of Schistosoma haematobium. *Nature* **351**, 757-759 (1991).
14. P. Zhang, Z. Feng, F. Milner, A schistosomiasis model with an age-structure in human hosts and its application to treatment strategies. *Mathematical Biosciences* **205**, 83-107 (2007).
15. J. C. Buck, W. J. Ripple, Infectious agents trigger trophic cascades. *Trends in ecology & evolution* **32**, 681-694 (2017).
16. C. J. E. Haggerty *et al.*, Aquatic macrophytes and macroinvertebrate predators affect densities of snail hosts and local production of schistosome cercariae that cause human schistosomiasis. *PLOS Neglected Tropical Diseases* **14**, e0008417 (2020).